Soft Matter

Accepted Manuscript

This article can be cited before page numbers have been issued, to do this please use: K. Nakao, A. Steinhauser, G. Durand, M. Soulié, G. N. Rechberger, T. Züllig, S. Keller and K. M. Tych, *Soft Matter*, 2025, DOI: 10.1039/D5SM00327J.

ROYAL SOCIETY OF CHEMISTRY

rsc.li/soft-matter-journal

View Article Online
DOI: 10.1039/D5SM00327J

Soft Matter

ARTICLE TYPE

Cite this: DOI: 00.0000/xxxxxxxxxx

Home is Where the Lipids Are: A Comparison of MSP and DDDG Nanodiscs for Membrane Protein Research†

Kaori Nakao[a‡] Alexandra Steinhauser[b‡], Grégory Durand[c], Marine Soulié[c], Gerald N. Rechberger[b], Thomas Züllig[b], Sandro Keller[*b] and Katarzyna Tych[*a]

Received Date
Accepted Date

DOI: 00.0000/xxxxxxxxxx

Nanodiscs have emerged as a powerful tool for studying membrane proteins in a lipid bilayer, with the standard approach relying on MSP-based nanodiscs that use detergent-mediated lipid exchange and encapsulation by MSP rings. However, this method may introduce artefacts from MSP interactions with the target protein and the nanodiscs' constrained size. Here, we compare MSP-based nanodiscs with an alternative system using the amphiphile dodecyl-diglucoside (DDDG), which directly extracts membrane proteins along with their surrounding lipids from the cell membrane. Using a glutamate transporter homolog (GltTk) from *Thermococcus kodakarensis* as a model, we assessed the efficiency of extraction and purification, thermal stability, and substrate binding capacity of GltTk in each of the two nanodisc systems. Our findings demonstrate that DDDG-based nanodiscs are comparable to MSP-based nanodiscs but may provide greater conformational flexibility and avoid possible artefacts due to MSP-GltTk interactions. Consequently, they provide a competent alternative to MSP-based nanodiscs through direct extraction, thereby preserving the proteins' native lipid environment. Both approaches support structural and functional studies, but their suitability depends on the specific application. MSP-based nanodiscs remain advantageous for studies requiring well-defined lipid compositions, while DDDG nanodiscs offer distinct advantages for investigating proteins where native lipids and conformational freedom are critical.

Introduction

Membrane proteins are essential for a broad spectrum of physiological functions. Representing approximately 30% of all proteins encoded by the human genome, they mediate essential intra- and transcellular molecular interactions [2]. Their surfaces exhibit hydrophobic properties, resulting in their instability when exposed to water. Consequently, in their purified state, they are incompatible with numerous tools employed in *in vitro* biochemical studies. To address this challenge, detergents with a range of properties have been developed and used for decades. More recently, a variety of nanodiscs have emerged as a novel tool for studying these fascinating proteins. These soluble discoidal lipid bilayer patches enable diverse experimental applications.

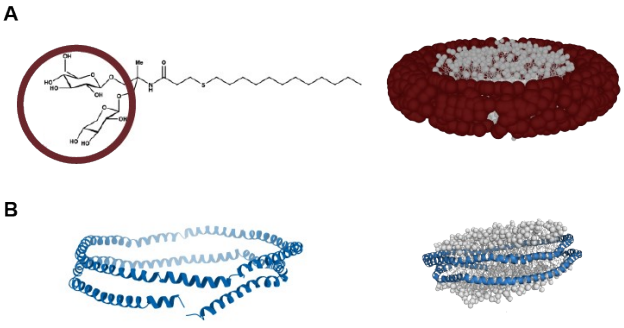

Fig. 1 DDDG- and MSP-based nanodiscs in this study A: DDDG-based nanodiscs are formed by direct extraction of membrane proteins and native lipids from membranes. B: MSP nanodiscs are assembled by reconstituting purified membrane proteins into a defined lipid bilayer stabilized by MSPs. Figures were generated based on PDB ID: 6CLZ[1].

Membrane scaffold proteins (MSPs) were first introduced in the early 2000s as a versatile platform for stabilizing membrane proteins in a native-like lipid bilayer environment [3]. In an MSP-based nanodisc, a pair of alpha helical proteins derived from a

[a] *Groningen Biomolecular Sciences and Biotechnology Institute, University of Groningen, Nijenborgh 7, 9747 AG Groningen, the Netherlands. ∗E − mail : k.m.tych@rug.nl*
[b] *Institut für Molekulare Biowissenschaften (IMB), Humboldtstr. 46–50, 8010 Graz, Austria. ∗E − mail : sandro.keller@uni − graz.at*
[c] *Avignon University, 301 rue Baruch de Spinoza, 84916 Avignon cedex 9, France*
‡ These authors contributed equally to this work
† Supplementary Information available: [The supplementary information includes data on protein yields in DDDG, DDM, and MSP, results from Western blot and size exclusion chromatography, as well as lipid detection analyses performed using FULL-MDS and mass spectrometry.]. See DOI: 10.1039/cXsm00000x/

View Article Online
DOI: 10.1039/D5SM00327J

human apolipoprotein A-1 form and retain certain sizes of a discoidal patch of lipids in solution. Although alternative protein-based nanodisc systems have been developed since then - such as salipro[4] and constructs based on short amphipathic peptides[5–8] - MSPs remain the most widely used, especially in structural biology, where they have greatly contributed to developments in cryo-electron microscopy[9]. Nanodiscs have opened possibilities to study lipid- protein interactions in addition to aiding in overcoming issues related to the poor stability of membrane proteins. Extensive protein engineering and open science initiatives have resulted in a range of MSP constructs with different molecular weights [10–12]. This diversity allows researchers to select an MSP variant tailored to the size and conformational flexibility of their protein of interest, providing sufficient space for dynamic structural rearrangements. However, despite their widespread application and success, MSP nanodiscs have certain limitations. Their defined lipid composition and the size dictated by the scaffold protein may restrict flexibility when it comes to mimicking the complex lipid environments of native membranes. Moreover, interactions between the MSP rings and the reconstituted membrane protein may limit the activity or conformational transitions of the target protein[13]. Additionally, the standard workflow for generating MSP-based nanodiscs requires detergent extraction of the target protein and subsequent reconstitution. This long process could lead to problems such as the denaturation or aggregation of the protein of interest.

To overcome some of these limitations, alternative membrane-mimetic systems have been developed. In particular, lipid-solubilising polymers have emerged as promising alternatives due to their ability to directly extract membrane proteins from native membranes[14]. Commonly used copolymers such as styrene-maleic acid (SMA)[15], diisobutylene/maleic acid (DIBMA)[16] have been widely applied to directly extract membrane proteins from native membranes while maintaining their surrounding lipid environment. Similarly, small amphiphilic molecules offer an alternative approach by directly extracting membrane proteins from biological membranes while simultaneously forming nanodiscs[17,18].

For our experiments, we chose the glyco-amphiphile DDDG, as it has proven to be a promising tool for the direct extraction and purification of membrane proteins [17,18] (Figure 1). As an amphiphilic detergent, DDDG exhibits a critical micelle concentration (CMC) that must be maintained in all buffers to ensure effective extraction and nanodisc formation. The suitability of DDDG for extracting membrane proteins into lipid-bilayer nanodiscs has been demonstrated in several instances[17–19]. For example, DDDG enabled the extraction of the bacterial ABC transporter BmrA from *E. coli* and the human G protein-coupled receptor (GPCR) A2AR from Sf9 insect cells, achieving higher solubilization efficiencies than the commonly used detergent DDM[17]. In a subsequent study, DDDG was shown to solubilize reconstituted proteoliposomes containing outer membrane phospholipase A (OmpLA) and to form nanodiscs directly from native membranes[18]. Due to the direct extraction from native membranes, DDDG nanodiscs often incorporate a larger amount of lipids than classic detergents, resulting in generally larger and more variable nanodisc sizes. In contrast, MSP nanodiscs offer a well-defined and uniform size. DDDG nanodiscs incorporate native lipid compositions directly extracted from target-protein expressing *E. coli* membranes, in contrast to the defined, synthetic lipid mixtures typically used for reconstitution in MSP nanodiscs. This inherent heterogeneity creates a more native-like lipid environment that can allow for greater conformational freedom of membrane proteins and their associated lipids. Moreover, solubilising target proteins with a variety of lipid species may help preserve the functional and structural integrity of these proteins.

To investigate how different lipid environments affect membrane protein purification and function, we compared DDDG and MSP1E3D1[10] nanodiscs as two distinct "homes" for a membrane transporter. As a model protein, we used GltTk, a glutamate transporter homolog from *Thermococcus kodakarensis*[20]. GltTk forms trimers that are fully embedded in the lipid bilayer and operates via an elevator mechanism, in which one domain slides relative to the other[21]. Our study shows how different nanodisc compositions influence the purification efficiency, sample heterogeneity, ligand binding, and thermal stability of this transporter.

Results and Discussion

DDDG forms larger nanodiscs compared to MSP1E3D1.
To assess differences arising from the nanodisc formation methods, we first compared extraction efficiencies and subsequent protein yields. GltTk was successfully extracted with both dodecyl-β-D-maltopyranoside (DDM) and DDDG (Figure S1). However, the subsequent reconstitution of the DDM-solubilized sample into MSP1E3D1 nanodiscs resulted in a noticeable loss of protein, likely due to the multiple processing steps required. In contrast, direct extraction with DDDG enabled the formation of nanodiscs without reconstitution, resulting in substantially increased yields (approximately 30-fold) compared to MSP nanodiscs (Figure S2). In the subsequent size-exclusion chromatography (SEC), the main peak eluted earlier than expected from the molecular weight of GltTk trimer (Figure S3). This earlier elution suggests an increased hydrodynamic radius, which may result from additional lipids incorporated into the nanodiscs or from nanodiscs associating with each other[18]. This effect was particularly noticeable in the DDDG preparation, reflecting its ability to extract membrane proteins together with a substantial portion of their native lipid environment. Using fluorescent universal lipid labeling (FULL-MDS)[19], we confirmed the presence of lipids in DDDG nanodiscs (Figure S4). Further lipidomic analysis by mass spectrometry (MS) identified typical *E. coli* lipids, including phosphatidylglycerol (PG), phosphatidylethanolamine (PE), cardiolipin (CL), and acyl phosphatidylglycerol (AcylPG)(Figure 2).

Notably, DDDG preserved the native lipid environment around GltTk, as the lipid composition in the nanodiscs closely resembled that of the original membrane vesicles from which they were extracted. Moreover, negative-staining electron microscopy revealed that GltTk-containing DDDG nanodiscs exhibit a significantly larger average diameter ((25.0 ± 5) nm) compared to MSP1E3D1 nanodiscs ((13.5 ± 1) nm) (Figure 3). In addition to

View Article Online
DOI: 10.1039/D5SM00327J

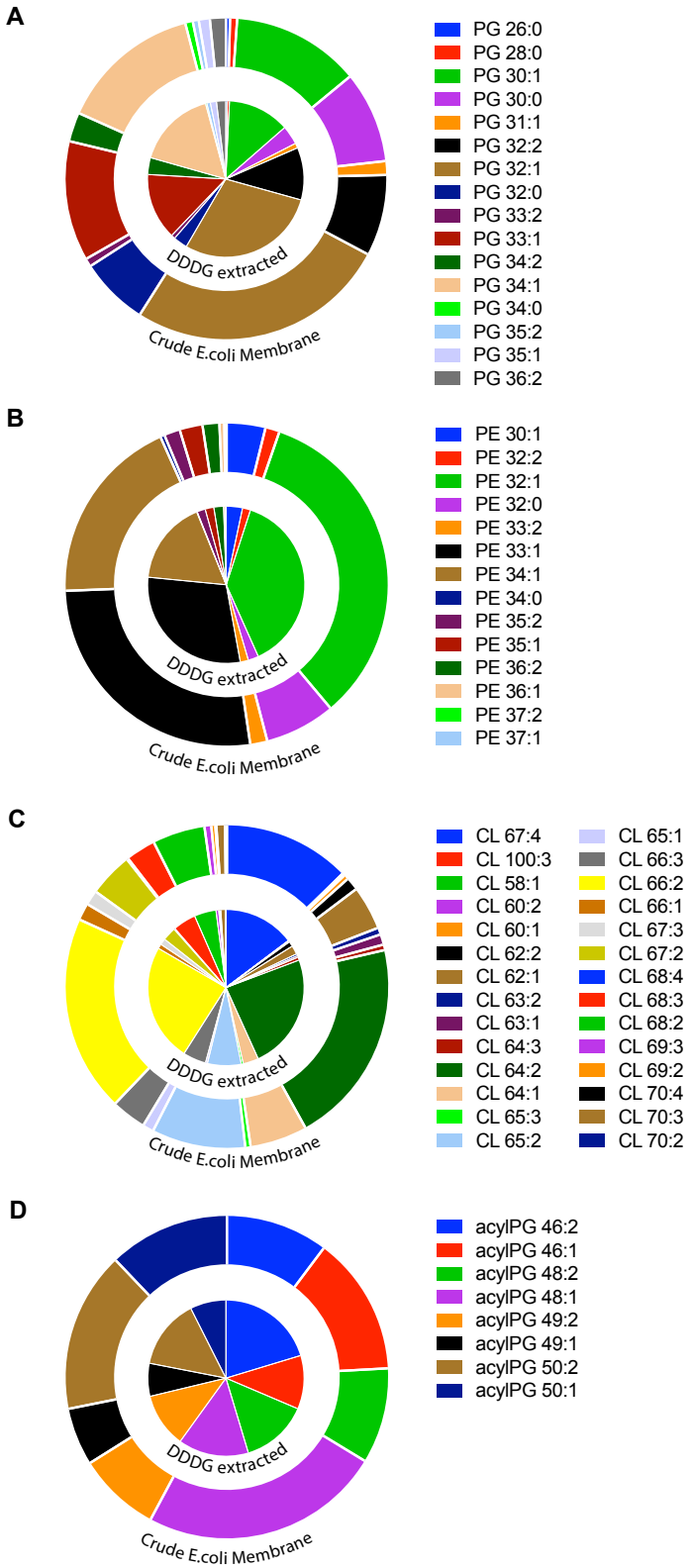

Fig. 2 Lipid species identified in crude *E. coli* membrane (outer circle) and GltTk-DDDG nanodiscs (inner circle). A: phosphatidylglycerol (PG), B: phosphatidylethanolamine (PE), C: cardiolipin (CL), and D: acyl phosphatidylglycerol (AcylPG) The numeric values following the lipid abbreviations indicate the total number of carbon atoms and double bonds in the fatty acyl chains.

the increased mean diameter, the DDDG nanodiscs also displayed a broader size distribution, as expected from the self-assembly properties of a small-molecule amphiphile. Similar size heterogeneity has been reported for lipid-solubilizing polymers such as SMA or DIBMA, which also extract membrane proteins directly with their native lipid environment [14–16]. Consequently, this native extraction approach leads to greater variability in nanodisc size compared to the more uniform assemblies formed with MSPs.

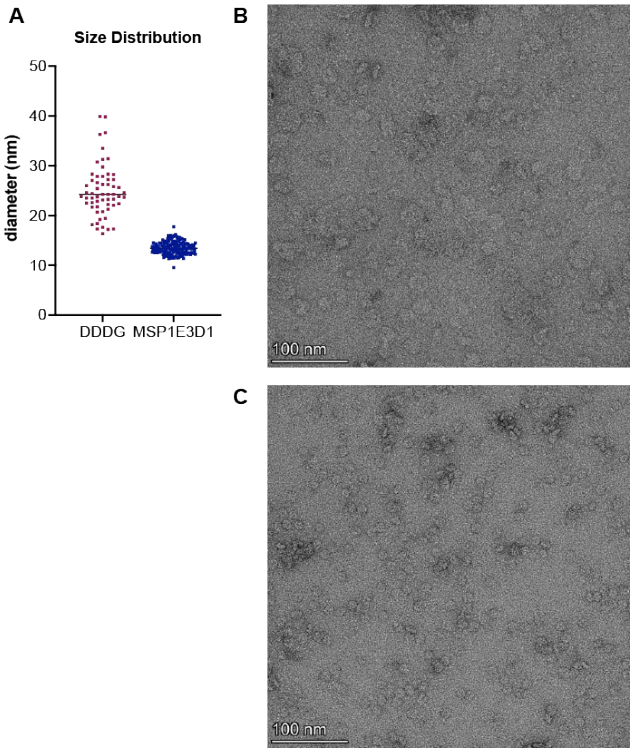

Fig. 3 Size distributions of nanodiscs determined by negative-staining electron microscopy. A: Comparison of nanodisc diameters measured from negative-staining electron microscopy images. GltTk-DDDG nanodiscs were found to have a mean diameter of 25.0 (± SD 5) nm, whereas MSP1E3D1 nanodiscs were found to have a mean diameter of 13.5 (±SD 1) nm. Measurements of the diameters for 59 particles in micrograph (B), 155 in (C) were performed in ImageJ. B,C: Example negative staining microscopy images for GltTk in (B) DDDG nanodiscs and (C) MSP1E3D1 nanodiscs. The scale bars represent 100 nm.

MSP1E3D1 nanodiscs containing GltTk exhibit a higher thermal stability.

We performed a thermostability assay (Figure 4), where GltTk was characterized in DDDG and MSP1E3D1 nanodiscs. GltTk remained more heat-stable in MSP compared to DDDG. The results revealed a clearly higher stability in the MSP1E3D1 nanodiscs. After incubation at 75°C for 30 min, no detectable band intensity remained in the DDDG sample, whereas approximately 60% of the initial band intensity was still present in the MSP1E3D1 sample. The absence of a band at the expected molecular weight after incubation at 75°C indicates that GltTk purified in DDDG undergoes thermal denaturation and aggregation, resulting in the loss of detectable protein. In contrast, GltTk reconstituted in MSP1E3D1 nanodiscs exhibits increased thermal stability, as

View Article Online
DOI: 10.1039/D5SM00327J

the protein remains detectable at 75°C, indicating better preservation of its structural integrity under heat stress. The increased stability of GltTk in MSP1E3D1 nanodiscs is likely due to the enhanced structural support and protection they provide, compared to the less stabilizing environment of DDDG.

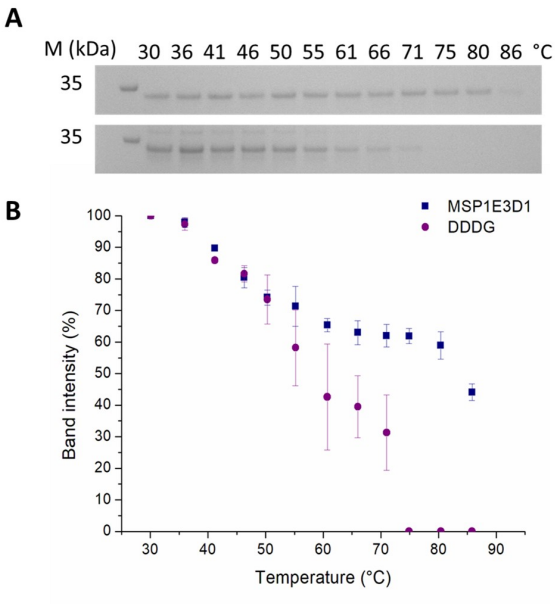

Fig. 4 GltTk remains thermally more stable in MSP1E3D1 compared to DDDG. A: Purified protein in MSP1E3D1 (top) and DDDG (bottom) was diluted to 120 ng/µL and incubated at temperatures between 30°C and 85°C for 30 min. B: Band intensity plotted as a function of temperature. Quantification was performed using ImageJ.

Substrate binding affinity of GltTk is higher in DDDG than in MSP1E3D1.

In order to compare functional aspects of GltTk in both, DDDG and MSP1E3D1 nanodiscs, we probed its substrate-binding capacity in both nanodisc environments. The binding of GltTk to its substrate, aspartate, was measured using a scintillation proximity assay (Figure 5)[22]. Here, radiolabelled substrates are detected on the surface of scintillant-containing beads, when they bind via immobilised protein. In DDDG nanodiscs, GltTk appears to bind to aspartate tighter (with a higher affinity, i.e., lower measured dissociation constant at K_D 54.2 nM, Figure 5A) than in MSP nanodiscs (K_D 205 nM, (Figure 5B)). Interestingly, these affinity values are significantly different from those measured in detergent (K_D 6.58 nM), suggesting that the lipid environment may play a pivotal role in modulating substrate binding. The lipid composition derived from recombinant cells in DDDG nanodiscs likely promotes favourable lipid-protein interactions with GltTk, enhancing its function and potentially stabilising active states. These findings underscore the critical importance of selecting an appropriate membrane-mimetic system when characterising membrane proteins in vitro, as even subtle variations in lipid-protein interactions can lead to significant differences in functional outcomes.

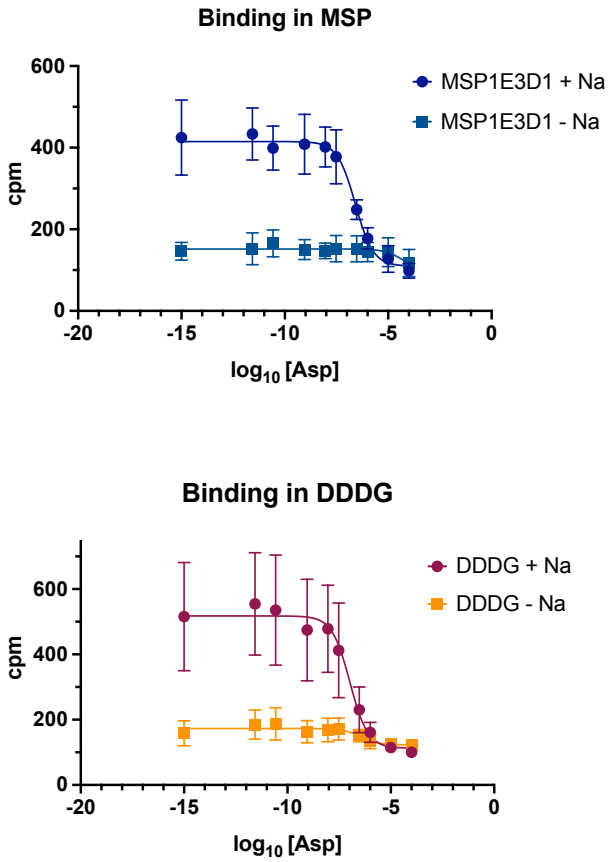

Fig. 5 Binding of GltTk to aspartate measured with a scintillation proximity assay. GltTk exhibits binding in the presence of sodium in both types of nanodiscs, in agreement with its previously reported activity as sodium symporter. Error bars are from biological duplicates, each with technical triplicates.

Experimental Methods

GltTk production

Recombinant GltTk with a single amino acid mutation from histidine 334 to cysteine was expressed in *E.coli* MC1061 in LB medium containing 100 μg mL^{-1} ampicillin (Foremedium) at 37°C, as described previously. [23] Briefly, once optical density at 600 nm (OD600) reached 0.8, protein expression was induced with 0.05% L-arabinose (Sigma Aldrich) and the culture was continued shaken for 3 h. Cells were collected by centrifugation at 6,000 x g at 4°Cfor 20 min and resuspended in 50 mM Tris-HCl pH 8.0, 300 mM KCl. After breaking cells under the presence of DNase A, 1 mM $MgSO_4$, 200 μM Phenylmethylsulfonyl fluoride (PMSF) at 25 kPsi, cell lysate was centrifuged to remove cell debris at 17,418 x g for 30 min, then the membrane fraction was collected by ultracentrifugation (Beckmann Coulter) at 186,000 x g, 4°C for 150 min.

GltTk extraction and purification by DDDG

The synthesis of DDDG was carried out as described in [17]. 10.1 mM DDDG and 200 μM PMSF were added to crude membrane vesicles in buffer A (50 mM Tris-HCl pH 8.0, 300 mM KCl, 1 mM

View Article Online
DOI: 10.1039/D5SM00327J

dithiothreitol (DTT)) and the mixture was incubated overnight on a rotary wheel. After ultracentrifugation (Beckmann Coulter) for 35 min at 80,000 rpm, the supernatant was incubated with Nickel resin equilibrated with 50 mM Tris-HCl pH 8.0, 300 mM KCl for 2.5 h under nutation. The sample was applied to an Nickel immobilized metal-ion affinity chromatography (Ni-IMAC), washed with buffer A supplemented with 200μM PMSF, 0.1 mM DDDG, and 50 mM imidazole pH 8.0, then eluted in one with 0.1 mM DDDG and 400 mM imidazole pH 8.0. After Ni-IMAC, the sample was desalted using PD10 column (Cytiva). Fractions were pooled and concentrated before being applied to a Superose 6 column (Cytiva).

Production and purification of MSP1E3D1

MSP was prepared following the protocol introduced, substituting NaCl with KCl[24]. The gene encoding MSP1E3D1 with the N-terminal polyhistidine-tag in pET28a plasmid (Addgene) was transformed into *E. coli* BL21 (DE3) cells. Cells were grown in TB medium under high oxygenation and the presence of 10 μg/mL of kanamycin at 37°C. Once OD600 reached 2, expression was induced with 1 mM Isopropyl β-d-1-thiogalactopyranoside (IPTG). Cells were collected after 3 h by centrifugation and resuspended in 50 mM Tris-HCl, pH 7.5, 300 mM KCl and stored at −70°C. For purification cells were allowed to thaw and supplemented with 100 μg/mL DNase A, 1 mM $MgSO_4$, 200 μM PMSF and 1% of Triton X-100. Cells were disrupted with sonication (72 cycles, each 5 s pulse at 70% amplitude, separated by 5 s cooling intervals on ice). After centrifugation at 30,000 × g for 30 min at 4°C, the supernatant was supplemented with 20 mM imidazole, pH 8.0, and MSP1E3D1 was purified with Ni-IMAC. The resin was washed three times with 40 mM Tris-HCl, pH 8.0, 300 mM KCl, supplemented first with 1% Triton X-100, then 50 mM sodium cholate and 20 mM imidazole and finally 50 mM imidazole, pH 8.0 . MSP was eluted in 40 mM Tris-HCl, pH 8.0, 300 mM KCl, 500 mM imidazole. Fractions were pooled, supplemented with 5 mM ethylenediaminetetraacetic acid potassium salt (K-EDTA) and 1:40 w/w tobacco etch virus protease with a point mutation (TEV-S219V, [25] for tag cleavage for 90 min. The mixture was transferred to a 3.5 kDa MWCO membrane tube (Spectrum) and dialysed against 20 mM Tris-HCl, pH 8.0, 100 mM KCl, 0.5 mM K-EDTA, 0.5 mM DTT overnight at 4°C. The sample was added to Ni-IMAC resin and collected in the flow-through fraction with 20 mM Tris-HCl, pH 8.0, 100 mM KCl.

GltTk extraction and purification with a detergent and reconstitution into MSP1E3D1

1% w/v DDM (Glycon) and 200 μM PMSF was added to crude membrane vesicles in buffer A (50 mM Tris-HCl pH 8.0, 300 mM KCl, 1 mM DTT) and the mixture was incubated on ice for 1 h. Purification with Ni-IMAC was performed in a similar way as in DDDG substituting DDDG with 0.05% DDM, except incubation with the resin was on ice for 45 min. Fractions containing high concentration of the target was applied to NAP10 desalting column (Cytiva) equilibrated with the buffer B (50 mM Tris-HCl pH7.5, 150 mM KCl, 1 mM DTT) with 0.05% DDM. *E.coli* polar lipids and Egg PC (3:1, Avanti Polar Lipids) were sonicated and incubated with 30 mM DDM to solubilise. The amounts of protein monomer, solubilized lipids, MSP were calculated so the molar ratio is to be 3:5:250. GltTk and lipids were mixed and incubated on ice for 30 min, MSP was added to be nutated together for another 30 min, and finally hydrolized Biobeads (Biorad) were added to the mixture and incubated overnight to remove detergents. After removing Biobeads and spinning down to remove precipitants, the reconstitution mixture was applied to a Superdex 200 column (Cytiva) in buffer B.

Mass spectrometry

To identify differences of lipid composition between DDDG nanodiscs and *E.coli* membrane vesicles, we used an untargeted lipidomics approach utilizing a reversed-phase UHPLC-QToF system (Infinity II, 6560B, Agilent, Waldbronn, Germany). The following samples were analyzed: Sample 1 - DDDG nanodiscs (0.3 mg/mL), Sample 2 - *E.coli* membrane vesicles (0.3 mg/mL), and as controls (Supplementary information), Sample 3 - 50 mM Tris, 150 mM KCl, pH 8 + 0.1 mM DDDG, and Sample 4 - 50 mM Tris, 150 mM KCl, pH 8. These samples were extracted using an adapted version of the lipid extraction protocol[26]. The mobile phase consisted of a gradient of solvent A (water) and solvent B (isopropanol), both containing 1% formic acid, 10 mM ammonium formate, and 7.7 μM phosphoric acid to achieve effective separation of the lipid species. Data acquisition was performed in a data-dependent manner, allowing for the identification of lipids based on their mass-to-charge ratios (m/z) and fragmentation patterns. The mass spectrometer was operated in negative ionization mode to capture a comprehensive phospholipid profile. Lipid annotation was conducted using MS-Dial[27] software for database comparison and Skyline[28] for integration. Further data transformation was performed using R/RStudio and tidyversel[29].

Negative staining electron microscopy

Grids coated with a carbon film were glow discharged. Protein solution was loaded onto the grid and blotted after 1 minute to remove the excess of liquid with filter paper. The sample was stained with 1-2% uranyl acetate, pH 3.5. After 20 sec, the grid was blotted again and left to dry in air. Micrographs were acquired in a Talos L120c, (Thermo Scientific) operated at 120 keV. Diameters of nanodiscs were measured in ImageJ.

Thermostability assay

GltTk in both, MSP1E3D1 and DDDG nanodiscs was diluted to a concentration of 120 ng/μL in 50 mM Tris (pH 8), 150 mM KCl (supplemented with 0.1 mM DDDG for DDDG samples), and incubated for 30 min at temperatures from 30 to 85°Cin a thermal cycler (Eppendorf). Following this, the samples were centrifuged at 20,000 x g for 40 min to remove aggregates. Thereafter, a total of 900 ng of each sample was loaded onto an SDS-PAGE. Protein band quantification was performed using ImageJ. The error bars represent the standard deviation from triplicates.

View Article Online
DOI: 10.1039/D5SM00327J

Scintillation proximity assays (SPA)

GltTk in DDDG or MSP1E3D1 were both prepared in 50 mM Tris-HCl pH 7.5, 150 mM KCl, 100 μM tris(2-carboxyethyl)phosphine (TCEP), supplemented with 0.1 mM DDDG for DDDG samples. Final 50 nM protein, 300 mM NaCl, serial concentrations of cold asp and 500 pM [^{3}H] labelled L-Asp were added to YSi copper His tag SPA beads suspension (revvity). After 1 h of incubation, scintillation was counted in a 96 well plate.

Conclusions

Our results show clear differences between MSP and DDDG nanodiscs in terms of extraction efficiency, size, thermal stability, and substrate-binding affinity. DDDG enables the direct extraction of transmembrane proteins from native environments while simultaneously forming nanodiscs, offering physiologically relevant lipid composition as well as a facilitated process compared to MSP-based systems. For GltTk, extraction into DDDG nanodiscs resulted in higher yields too. However, these advantages do not mean that DDDG is the best option in every situation. The heterogeneity observed in our negative staining data may complicate initial image analysis. In that sence, the homogeneity in the size distribution provided by MSP would be a better starting point for electron microscopy-based structural work. MSP opens possibilities to systematic investigations of lipid-dependent effects by allowing the use of specific lipid mixtures for reconstitution.

The enhanced thermal stability observed in GltTk in MSP1E3D1 nanodiscs could be influenced by an increased conformational stability of the protein, in addition to potential detergent-related artifacts. Variations in lipid composition between the two nanodisc systems are also likely to play a role. Here, the dynamic nature of DDDG nanodiscs — which manifests in fast lipid exchange[18] and may also mimic the fluidity of lipid bilayer— enables interaction studies within a "home" environment. Overall, these findings highlight DDDG nanodiscs as versatile tools for studying diverse membrane proteins in physiologically relevant lipid environments. It should be noted, however, that our findings are based on a single membrane protein, GltTk, and thus their applicability to proteins with distinct structures or biophysical characteristics remains to be validated.

Author contributions

SK, KT, and KN designed the experiments. KN and AS performed the experimental work. GD and MS synthesized research chemicals. GR and TZ performed the mass spectrometry measurements.

Conflicts of interest

DDDG is available at Eurofins CALIXAR under the trade name Xtract-DDDG.

Data availability

The data supporting this article have been included as part of the Supplementary Information. Raw data have been deposited in Figshare and are available under
DOI: 10.6084/m9.figshare.29434493

Acknowledgements

We thank M.C.A Stuart (University of Groningen) for negative-staining electron microscopy imaging, M. van den Noort (University of Groningen) for MSP nanodisc preparations. We are also grateful to L. Bauernhofer (University of Graz) for scientific discussions and valuable input.

Notes and references

1 T. C. Marcink, J. A. Simoncic, B. An, A. M. Knapinska, Y. G. Fulcher, N. Akkaladevi, G. B. Fields and S. R. Van Doren, *Structure*, 2019, **27**, 281–292.e6.
2 E. Wallin and G. V. Heijne, *Protein Science*, 1998, **7**, 1029–1038.
3 T. H. Bayburt, Y. V. Grinkova and S. G. Sligar, *Nano Letters*, 2002, **2**, 853–856.
4 J. Frauenfeld, R. Löving, J.-P. Armache, A. F.-P. Sonnen, F. Guettou, P. Moberg, L. Zhu, C. Jegerschöld, A. Flayhan, J. A. G. Briggs, H. Garoff, C. Löw, Y. Cheng and P. Nordlund, *Nature Methods*, 2016, **13**, 345–351.
5 M. L. Carlson, J. W. Young, Z. Zhao, L. Fabre, D. Jun, J. Li, J. Li, H. S. Dhupar, I. Wason, A. T. Mills *et al.*, *Elife*, 2018, **7**, e34085.
6 T. Ravula, D. Ishikuro, N. Kodera, T. Ando, G. M. Anantharamaiah and A. Ramamoorthy, *Chemistry of Materials*, 2018, **30**, 3204–3207.
7 B. R. Sahoo, T. Genjo, S. J. Cox, A. K. Stoddard, G. Anantharamaiah, C. Fierke and A. Ramamoorthy, *Journal of Molecular Biology*, 2018, **430**, 4230–4244.
8 B. Krishnarjuna, G. Sharma, S.-C. Im, R. Auchus, G. M. Anantharamaiah and A. Ramamoorthy, *Journal of Colloid and Interface Science*, 2024, **653**, 1402–1414.
9 S. G. Sligar and I. G. Denisov, *Protein Science*, 2020, **30**, 297–315.
10 I. G. Denisov, Y. V. Grinkova, A. A. Lazarides and S. G. Sligar, *Journal of the American Chemical Society*, 2004, **126**, 3477–3487.
11 T. H. Bayburt and S. G. Sligar, *FEBS Letters*, 2009, **584**, 1721–1727.
12 Y. V. Grinkova, I. G. Denisov and S. G. Sligar, *Protein Engineering Design and Selection*, 2010, **23**, 843–848.
13 V. Dalal, M. J. Arcario, J. T. Petroff, B. K. Tan, N. M. Dietzen, M. J. Rau, J. A. Fitzpatrick, G. Brannigan and W. W. Cheng, *Nature communications*, 2024, **15**, 25.
14 J. F. Bada Juarez, A. J. Harper, P. J. Judge, S. R. Tonge and A. Watts, *Chemistry and Physics of Lipids*, 2019, **221**, 167–175.
15 T. J. Knowles, R. Finka, C. Smith, Y.-P. Lin, T. Dafforn and M. Overduin, *Journal of the American Chemical Society*, 2009, **131**, 7484–7485.
16 A. O. Oluwole, J. Klingler, B. Danielczak, J. O. Babalola, C. Vargas, G. Pabst and S. Keller, *Langmuir*, 2017, **33**, 14378–14388.
17 P. Guillet, F. Mahler, K. Garnier, G. Nyame Mendendy Boussambe, S. Igonet, C. Vargas, C. Ebel, M. Soulié, S. Keller, A. Jawhari and G. Durand, *Langmuir*, 2019, **35**, 4287–4295.

View Article Online
DOI: 10.1039/D5SM00327J

18 F. Mahler, A. Meister, C. Vargas, G. Durand and S. Keller, *Small*, 2021, **17**, 2103603.

19 J. Baron, L. Bauernhofer, S. R. A. Devenish, S. Fiedler, A. Ilsley, S. Riedl, D. Zweytick, D. Glueck, A. Pessentheiner, G. Durand and S. Keller, *Analytical Chemistry*, 2022.

20 D. J. Slotboom, W. N. Konings and J. S. Lolkema, *Microbiology and Molecular Biology Reviews*, 1999, **63**, 293–307.

21 A. A. Garaeva and D. J. Slotboom, *Biochemical Society Transactions*, 2020, **48**, 1227–1241.

22 D. S. Auld, M. W. Farmen, S. D. Kahl, A. Kriauciunas, K. L. McKnight, C. Montrose and J. R. Weidner, *Assay Guidance Manual [Internet]*, 2018.

23 V. Arkhipova, A. Guskov and D. J. Slotboom, *Nature communications*, 2020, **11**, 998.

24 T. Ritchie, Y. Grinkova, T. Bayburt, I. Denisov, J. Zolnerciks, W. Atkins and S. Sligar, in *Reconstitution of Membrane Proteins in Phospholipid Bilayer Nanodiscs*, Elsevier, 2009, pp. 211–231.

25 S. C. Joseph E. Tropea and D. S. Waugh, *High Throughput Protein Expression and Purification: Methods and Protocols*, Humana Press, 2009.

26 V. Matyash, G. Liebisch, T. V. Kurzchalia, A. Shevchenko and D. Schwudke, *Journal of Lipid Research*, 2008, **49**, 1137–1146.

27 H. Tsugawa, K. Ikeda, M. Takahashi, A. Satoh, Y. Mori, H. Uchino, N. Okahashi, Y. Yamada, I. Tada, P. Bonini, Y. Higashi, Y. Okazaki, Z. Zhou, Z.-J. Zhu, J. Koelmel, T. Cajka, O. Fiehn, K. Saito and M. Arita, *Nature Biotechnology*, 2020, **38**, 1159–1163.

28 B. MacLean, D. M. Tomazela, N. Shulman, M. Chambers, G. L. Finney, B. Frewen, R. Kern, D. L. Tabb, D. C. Liebler and M. J. MacCoss, *Bioinformatics*, 2010, **26**, 966–968.

29 H. Wickham, M. Averick, J. Bryan, W. Chang, L. D. McGowan, R. François, G. Grolemund, A. Hayes, L. Henry, J. Hester, M. Kuhn, T. L. Pedersen, E. Miller, S. Bache, K. Müller, J. Ooms, D. Robinson, D. Seidel, V. Spinu and H. Yutani, *Journal of Open Source Software*, 2019, **4**, 1686.

The data supporting this article have been included as part of the Supplementary Information. Raw data have been deposited in Figshare and are available under DOI: 10.6084/m9.figshare.29434493